Chiang Mai J. Sci. 2021; 48(5) : 1412-1429
http://epg.science.cmu.ac.th/ejournal/
Contributed Paper

Mathematical Modeling of the Gyrotactic Microorganisms of non Darcian Micropolar Fluid Containing Different Nanoparticles

Nabil T Eldabe [a], Mahmoud E. Gabr [b], Khalid K. Ali [c], Sameh Abdelzaher [b] and A.Z. Zaher*[d]

[a] Mathematics Department, Faculty of Education, Ain Shams University, Egypt
[b] Mathematics Department, Faculty of Science, Zagazig University, Egypt
[c] Mathematics Department, Faculty of Science, Al-Azhar University, Nasr-City Cairo, Egypt
[d] Engineering Mathematics and physics Department, Faculty of Engineering-Shubra Benha University, Egypt

*Author for correspondence; e-mail: abdullah.zaher@feng.bu.edu.eg

Received: 12 October 2020
Revised: 22 January 2021
Accepted: 8 March 2021

Abstract

In this study, we consider the non-Darcian model of Gyrotactic Microorganisms and electro-magnetohydrodynamic (EMHD) for micropolar bio viscos fluid containing different kinds of nanoparticles over a stretching plate. The problem is formulated mathematically by a system of non-linear partial differential equations (PDEs). By using suitable transformations, the PDEs system is transformed into a system of non-linear ordinary differential equations (ODE) subjected to appropriate boundary conditions. These equations are solved numerically by using the finite difference method. The model is applied to human blood, as a bio viscos fluid containing four different types of nano-particles such as Copper (Cu), Silver (Ag), aluminum oxide (Al_2O_3), and Titanium dioxide (TiO_2). The effects of some parameters on the obtained solutions are discussed numerically and illustrated graphically through a set of figures. The results showed that the momentum for Al_2O_3-nanoparticles and TiO_2-nanoparticles is spreading faster inside the blood than propagating momentum for Cu-nanoparticles, Ag-nanoparticles. The importance of this study comes from its significant applications in many scientific fields, such as nuclear reactors, medicine, and geophysics.

Keywords: boundary layer, micropolar fluid, nanoparticles, moving surface, electrical magnetic field, chemical reaction, heat and mass transfer, scientific computations, gyrotactic microorganisms

1. Introduction

The study of the behavior of Newtonian and non-Newtonian fluids flow is important for engineering and medical industries. Biological fluids such as blood fail to comply with Newton's viscosity law and are considered non-Newtonian fluids [1]. Recent experimental researches proved that nanofluids are more effective medium for thermal conductivity. Therefore, the heat transfer efficiency is expected to improve dramatically, incorporating both the advantages of bioconvection and nanofluid thermal conductivity. During the past few decades, nanomaterials have grasped the full attention of scientists as well as engineers. Nanomaterials are recognized to enhance the thermal conductivity of base fluids like water, ethylene glycol, etc. In 1995, Choi et al. [2] studied

nanofluids in the Argonne Federal Laboratory, USA. The nanoparticles used in nanofluids are typically made of metals, oxides, carbides, or element nanotubes. The importance of using the nanofluids is the enhancement of the heat transfer inside the base fluid. This is because those nanoparticles change the properties of the base fluid and enhancement of thermal conductivity and efficiency of the new fluid. Commonly utilized nanoparticles are metals (Cu, Ag, Fe) and metal oxides (CuO, Al_2O_3, TiO_2, Fe_3O_4 and ZnO). Enhanced thermal conductivity of nanofluids has satisfying applications not only in domestic heating but also, cooling systems, photovoltaic thermal systems, automobile engine industry, heat exchangers, radiation therapy, and more [3]. The unsteady flow over a continuously shrinking surface with wall mass suction in a water based nanofluid containing different type of nanoparticles: CuO, Al_2O_3 and TiO_2 is studied by Azizah et al.[4] They found that the flow and heat transfer are significantly influenced by the unsteadiness and the solid volume fraction parameters for the three different nanoparticles CuO, Al_2O_3 and TiO_2. Hamad [5] examined the convective flow and heat transfer of an incompressible viscous nanofluid past a semi-infinite vertical stretching sheet in the presence of a magnetic field. He deduced that the heat transfer rates decrease as the nanoparticle volume fraction increases and for a selected value of the nanoparticle volume fraction the heat transfer rates decreases as magnetic field parameter increases. More significant and important contributions can be found in [6-7].

Because of its important applications many researchers investigated aspects of the bioconvection problems in suspensions containing solid particles [8]. Kuznetsov [9] recently conducted a series of analyzes on the bioconvection of a nanofluid in a suspension containing both nanoparticles and microorganisms. He found that the introduction of gyrotactic microorganisms to nanofluids is likely to improve as a suspension of their stability. He also found that suspensions of gyrotactic microorganisms may exhibit bioconvection, which is a macroscopic movement in the fluid caused by swimming or the movement of motile microorganisms. This is because the motile microorganisms are typically heavier than water so that in response to stimuli such as gravity, light, and chemical attractions they will move in the upward direction. Relevant studies include Alsaedi et al. [10] who also considered stratification effects of Magneto hydrodynamic (MHD) bioconvective flow of nanofluid due to gyrotactic microorganisms. Zohra et al. [11] who obtained slip, swirl and wall transpiration effects of magneto-bioconvection flow from a rotating cone to a Nanofluid with Stefan blowing effects. To this end, it is worth mentioning that, according to Vadasz [12], bioconvection may have contributed to the microsystems that are essential issues in many microsystems for the enhancement and mixing of mass transport.

Micropolar fluids are fluids consisting of rigid, randomly oriented, or (spherical) particles suspended in a viscous medium, where fluid deformation is ignored , studying this kinde of fluids required the consideration of the microscopic effects resulting from the local structure and micromotions of the fluid components. Micropolar fluid theory provides a mathematical model able to explain the non-Newtonian fluid behavior such as polymeric fluids, liquid crystals, paints, and animal blood. The microrotation of the suspended microparticles suspended inside the fluid is explored by micropolar fluid theory. Eringen [13] introduced the concept of simple micro fluids to describe condensed suspensions of neutrally buoyant deformable particles in a viscous fluid in which the identity of substructures influences the physical effect of the flow. Lok et al. [14] Investigated the theory of micropolar fluids by observing the behavior of the unsteady boundary layer flow of a micropolar fluid near the rear stagnation point of a plane surface. Sandeep and Sulochana [15] studied the unsteady mixed convection boundary flow of a micropolar fluid with uniform suction/injection over a stretching/

shrinking sheet. Also, influence of the thermal radiation interaction of the boundary layer flow of a micropolar fluid at a heated plate embedded in a porous medium with variable heat flux is considered by Rahman and Sultana [16].

The earlier studies of the Darcy model concentrated mostly on flow across porous media. To obtain accurate results for porous media with high permeability the non-Darcy model should be considered. Generally, when Temperature changes heat flux is produced and the came occurs when concentration is changed. These phenomena are called Soret and Dufour effects. These effects should be taken in consideration when studying important applications such as the solidification of binary alloys, groundwater pollutant migration, chemical reactors, geosciences multi-component melts, oil-reservoirs, isotope separation, and in mixture between gases. The study of Dufour and Soret effects are considered in many researches. Postelnicu [17] studied the heat and mass characteristics of natural convection on a vertical surface embedded in a saturated porous medium subjected to a magnetic field. Partha et al. [18] investigated the impact of Soret and Dufour effects in a porous non-Darcy medium, for more studies of Dufour and Soret effects see [19-21].

The main purpose of our study is to present a novel non-Darcian model for the Gyrotactic Microorganisms and electro-magnetohydrodynamic (EMHD) for micropolar bio viscos fluid containing different nanoparticles over a stretching surface. The human blood is taken as a base fluid and four different types of nano-particles, Copper (Cu), Silver (Ag), aluminum oxide (Al_2O_3) and Titanium dioxide (TiO_2) are added to the blood. Our study also concentrates on the Soret and Dufour effects, the impact of viscous dissipation, Joule heating, chemical reaction as well as heat and mass transfer. The problem is formulated mathematically by a system of non-linear partial differential equations (PDEs). Using suitable transformations this system is transformed into a non-linear system of ordinary differential equations (ODE) with appropriate boundary conditions. The finite difference method technique is used to obtain the numerical solution of the system.

2. MATHEMATICAL MODELING

Consider a steady two-dimensional flow of an incompressible micropolar biviscosity nanofluid over a linearly stretching sheet in a blood-based nanofluid containing four different types of nano-particles: Cu, Ag, Al_2O_3 and TiO_2. Assume $\underline{B} = (0, B_0, 0)$is the magnetic field acting normally on the stretching sheet. The fluid is electrically conducting and $\underline{E} = (0, 0, -E_0)$ is the electric field. The magnetic and electric fields obey Ohm's law $\underline{J} = \sigma(\underline{E} + \underline{V} \times \underline{B})$ where $\underline{J}$ is the Joule current, σ is the electrical conductivity and $\underline{V}$ represents the fluid velocity filed. The induced magnetic field can be neglected. The governing equations are the continuity equation, the momentum equation, the angular momentum equation, the energy equation, microorganism equation and the concentration equation. Also, Maxwell's and Ohm's law as well as the Brinkman-Forchheimer extended Darcy model [22] will be taken in consideration during this formulation.

The biviscosity model is [23]:

$$\tau_{ij} = \begin{Bmatrix} 2\left((\mu_B)_{nf} + \frac{p_y}{\sqrt{2\pi}}\right)e_{ij}, \pi \succ \pi_c \\ 2\left((\mu_B)_{nf} + \frac{p_y}{\sqrt{2\pi}}\right)e_{ij}, \pi \prec \pi_c \end{Bmatrix}. \quad (1)$$

Also introduce the non-dimensional parameter including:

$$\beta = \frac{(\mu_B)_{nf}\sqrt{2\pi_c}}{p_y}. \quad (2)$$

where μ_B is the plastic viscosity, p_y is the yielding stress, $\pi = e_{ij}e_{ij}$ where e_{ij} is the (i, j) component of the deformation rate and the value of β denotes the upper limit of apparent viscosity coefficient. Following Mekheimer et al. [24] and Brinkman [22] we can write the relationship between thermo-physical properties of base fluid and nano-particles as follows:

$$\mu_{nf} = \frac{\mu_f}{(1-\phi)^{2.5}}, \quad (3)$$

(Here, ϕ is the solid volume fraction of the nanoparticles, and μ_f is the dynamic viscosity of the base fluid)

$$(\rho)_{nf} = (1-\phi)(\rho)_f + \phi(\rho)_s, \quad (4)$$

$$(\rho c_p)_{nf} = (1-\phi)(\rho c_p)_f + \phi(\rho c_p)_s \quad (5)$$

$$\upsilon_{nf} = \frac{\mu_{nf}}{\rho_{nf}}, \quad (6)$$

$$\alpha_{nf} = \frac{k_{nf}}{(\rho c_p)_{nf}}, \quad (7)$$

$$\frac{k_{nf}}{k_f} = \frac{(k_s+k_f)-2\phi(k_f-k_s)}{(k_s+k_f)+\phi(k_f-k_s)}. \quad (8)$$

where k_{nf} is the thermal conductivity of the nanofluid, k_f and k_s are the thermal conductivities of the base fluid and of the nano particles respectively, ρ_s is the particles density, $(\rho c_p)_f$ and $(\rho c_p)_s$ are the heat capacity of the base fluid and the effective heat capacity of a nanoparticle, respectively, k_{nf} is the thermal conductivity of the nanofluid. The thermo-physical properties of the four types of the metallic nano-particles and blood are given in the following table:

3. BASIC EQUATIONS

Choose the Cartesian coordinate system such that x- axis along the stretching sheet and y-axis is taken normal to it, u and v are the fluid velocity components in the x and y - direction respectively. Assume the density of the motile microorganisms, temperature and nanoparticle volume fraction at the stretching surface are N_w, T_w and, C_w respectively, and those of the ambient nanofluid are N_∞, T_∞ and C_∞ respectively.

The two-dimensional electromagnetohydrodynamic (EMHD) boundary layer flow equations for the considered incompressible micropolar biviscosity Nanofluid can be written on the following form:

Continuity equation

$$\frac{\partial u}{\partial x} + \frac{\partial v}{\partial y} = 0, \quad (9)$$

Momentum equation

$$u\left(\frac{\partial u}{\partial x}\right) + v\left(\frac{\partial u}{\partial y}\right) = \frac{1}{\rho_{nf}}\left((\mu_B)_{nf}(1+\frac{1}{\beta}) + k^*\right)\frac{\partial^2 u}{\partial y^2} + \frac{k^*}{\rho_{nf}}\left(\frac{\partial N^*}{\partial y}\right) + \frac{\sigma}{\rho_{nf}}(E_o B_o - B^2{}_o u) - \frac{\upsilon_{nf}}{k}u - \frac{F}{k}u^2, \quad (10)$$

Angular momentum equation

$$\rho_{nf} j\left(u\frac{\partial N^*}{\partial x} + v\frac{\partial N^*}{\partial y}\right) = \gamma^*\frac{\partial^2 N^*}{\partial y^2} - k\left(2N^* + \frac{\partial u}{\partial y}\right) \quad (11)$$

Energy equation:

$$u\frac{\partial T}{\partial x} + v\frac{\partial T}{\partial y} = \alpha_{nf}\frac{\partial^2 T}{\partial y^2} + \tau_{nf}\left(D_B\frac{\partial c}{\partial y}\frac{\partial T}{\partial y} + \frac{D_T}{T_\infty}\left(\frac{\partial T}{\partial y}\right)^2\right) + \frac{1}{(\rho c)_{nf}}\left((\mu_B)_{nf}(1+\frac{1}{\beta}) + k^*\right)\left(\frac{\partial u}{\partial y}\right)^2 + \frac{\sigma}{(\rho c)_{nf}}(B_o u - E_o)^2 + \frac{D_m k_T}{C_s(c_p)_{nf}}\frac{\partial^2 c}{\partial y^2}. \quad (12)$$

Table 1. Physical properties of nanoparticles and blood.

Physical property	Blood	Cu	Ag	Al_2O_3	TIO_2
$\rho(m^{-3}Kg)$	1060	8933	10500	3970	4250
$C_p(K^{-1}JKg^{-1})$	3770	385	235	765	686.2
$k(K^{-1}Wm^{-1})$	0.492	401	429	40	8.9538
ϕ	0.000	0.05	0.10	0.15	0.20
$\sigma(s.m^{-1})$	4.3×10^{-5}	59.6×10^{6}	6.6×10^{-7}	3.5×10^{6}	2.6×10^{6}

Gyrotactic microorganism equation

$$u\frac{\partial N}{\partial x}+v\frac{\partial \mathrm{N}}{\partial y} = D_m\frac{\partial^2 \mathrm{N}}{\partial y^2}-\frac{bW_c}{C_w-C_\infty}\left(N\frac{\partial^2 C}{\partial y^2}+\frac{\partial \mathrm{N}}{\partial y}\frac{\partial C}{\partial y}\right) \quad (13)$$

Concentration equation

$$u\frac{\partial C}{\partial x}+v\frac{\partial C}{\partial y} = D_B\frac{\partial^2 C}{\partial y^2}+\frac{D_T}{T_\infty}\left(\frac{\partial^2 T}{\partial y^2}\right) + \frac{D_B k_T}{T_m}\frac{\partial^2 T}{\partial y^2}+k_\circ(C-C_\infty), \quad (14)$$

where u and v are the fluid velocity and the normal velocity components in the x and y orientations, respectively; υ_{nf}, ρ_{nf} and μ_{nf} are the nanofluid kinematic viscosity, nanofluid density and the effective dynamic viscosity of the nanofluid respectively; T, C, α_{nf} and $(\rho c_p)_{nf}$ are the temperature of the fluid in the boundary layer, fluid solutal concentration, the thermal diffusivity of the nanofluid and the nanofluid heat capacitance respectively; ρ, D_B, k_T, C_s, $(c_p)_{nf}$, T_m, k, F and $k_\circ$ are the density of the base fluid, the mass diffusivity of concentration, thermal diffusion ratio, concentration susceptibility, specific heat of the fluid at constant pressure, mean fluid temperature, permeability parameter, dimensional Forchheimer constant and the chemical reaction parameter, respectively. Where, k^* is the vortex viscosity coefficient, N^* is the component of the micro rotation vector $\vec{N}^*$ normal to the x, y – axes, j is the micro inertia density.

The spin gradient γ_{nf}^* can be defined as:

$$\gamma_{nf}^* = \left((\mu_B)_{nf}+\frac{k^*}{2}\right)j = \frac{(\mu_B)_f}{(1-\phi)^{2.5}}\left(1+(1-\phi)^{2.5}\frac{K}{2}\right)j \quad , (15)$$

where $K=\frac{k^*}{(\mu_B)_f}$ is the material parameter, $j=\frac{\upsilon_{nf}}{c}$ is the micro inertia constant.

The boundary conditions are as follows:

$$y=0: v=v_w,\ u=U_w(x)=cx,\ N^*=-n\frac{\partial u}{\partial y};$$
$$T=T_w, C=C_w, N=N_w,$$
$$y\to\infty: u\to 0, N^*\to 0, C\to C_\infty, T\to T_\infty, N\to N_\infty. \quad (16)$$

Where, c is the surface stretching constant and v_W its velocity.

Here for $k^*=0$ we retrieve the case of viscous fluid. The boundary parameter n has range $0\prec n\prec 1$. It should be noted that when n=0 (called strong concentration) then $N^*=0$ near the wall. This represents the concentrated particle flows in which the microelements close to the wall surface are unable to rotate. The case $n=1/2$ corresponds to the vanishing of antisymmetric part of the stress tensor and it shows weak concentration of microelements.

Introducing the nondimensional similarity transformations

$$\psi=\left(c\upsilon_f\right)^{\frac{1}{2}}xf(\eta),$$
$$\theta(\eta)=\frac{T-T_\infty}{T_w-T_\infty}, \varepsilon(\eta)=\frac{N-N_\infty}{N_w-N_\infty}$$
$$\Phi(\eta)=\frac{C-C_\infty}{C_w-C_\infty}; \eta=y\left(\frac{c}{\upsilon_f}\right)^{\frac{1}{2}},$$
$$N^*=c\left(\frac{c}{\upsilon_f}\right)^{\frac{1}{2}}xg(\eta) \quad (17)$$

where $\psi(x,y)$ is the stream function defined as

$$u=\frac{\partial\psi}{\partial y}=cxf'(\eta)\ ,\ v=-\frac{\partial\psi}{\partial x}=-\sqrt{c\upsilon_f}f(\eta)\ . \quad (18)$$

By using (17) and (18), the continuity equation is satisfied identically the governing equations (10), (11), (12), (13), (14) and (5) along with the boundary conditions (16) are reduced to the following nondimensional form:

$$\left((1+\frac{1}{\beta})+(1-\phi)^{2.5}K\right)f'''(\eta) + \phi_1\left(f(\eta)f''(\eta)-\left(1+\frac{F_s}{D_a}\right)(f'(\eta))^2\right) + K(1-\phi)^{2.5}g'(\eta)+M(1-\phi)^{2.5}\left(E_1-f'(\eta)\right) - \frac{1}{R_{ex}}\frac{1}{D_a}f'(\eta)=0, \quad (19)$$

$$\left(1+(1-\phi)^{2.5}\frac{K}{2}\right)g''(\eta)+\phi_1\big(f(\eta)g'(\eta) - f'(\eta)g(\eta)\big)-(1-\phi)^{2.5}\phi_1 K\big(2g(\eta) + f''(\eta)\big)=0, \quad (20)$$

$$(1-\phi)^{2.5}\theta''(\eta) + p_r\frac{k_f}{k_{nf}}\begin{pmatrix}\phi_2(1-\phi)^{2.5}f(\eta)\theta'(\eta)+\\(1-\phi)^{2.5}\big(N_b\theta'(\eta)\Phi'(\eta)+N_t\theta'(\eta)^2+D_u\Phi''(\eta)\big)\\+E_c\left((1+\frac{1}{\beta})+(1-\phi)^{2.5}K\right)(f''(\eta))^2\\+(1-\phi)^{2.5}ME_c(f'(\eta)-E_1)^2\end{pmatrix} = 0, \quad (21)$$

$$\varepsilon''(\eta)+Lb\varepsilon'(\eta)f(\eta)-P_e\big(\varepsilon'(\eta)\Phi'(\eta) + (\Omega+\varepsilon(\eta))\Phi''(\eta)\big)=0, \quad (22)$$

$$\Phi''(\eta)+\frac{N_t}{N_b}\theta''(\eta)+L_e(f(\eta)\Phi'(\eta) + \gamma\Phi(\eta)+S_r\theta''(\eta))=0. \quad (23)$$

Using the transformation (17) the boundary conditions (16) take the following form:

$$\begin{aligned}&f(0)=s, f'(0)=1, g(0)=-nf''(0),\\&\theta(0)=1,\Phi(0)=1,\varepsilon(0)=1\text{at }\eta=0;\\&f'(\eta)\to 0, g(\eta)\to 0,\theta(\eta)\to 0,\\&\Phi(\eta)\to 0,\varepsilon(\eta)\to 0: at\eta\to\infty.\end{aligned} \quad (24)$$

Here, f, θ, g, ε and Φ are the dimensionless velocity, temperature, dimensionless microrotation (angular velocity), dimensionless Gyrotactic microorganism and concentration, respectively, $M=\frac{\sigma {B_O}^2}{c\rho_f}$ is the magnetic field parameter, $E_1=\frac{E_0}{cxB_0}$ is the electric parameter, $F_s=\frac{F}{x}$ is the Forchheimer number, $D_a=\frac{k}{x^2}$ is the Darcy number and $R_{ex}=\frac{u_w(x)x}{\upsilon}$ the local Reynolds number. Here $p_r=\frac{\upsilon_f(\rho c)_f}{k_f}$ is the Prandtl number, $Nb=\frac{(\rho c)_p D_B(C_w-C_\infty)}{(\rho c)_f\upsilon_f}$ is the Brownian motion parameter, $Nt=\frac{(\rho c)_p D_T(T_w-T_\infty)}{T_\infty(\rho c)_f\upsilon_f}$ is the thermophoresis parameter, $D_u=\frac{D_m k_T(C_w-C_\infty)}{C_s(C_p)_f\upsilon_f(T_w-T_\infty)}$ is the Duffor number, $E_c=\frac{u_w^2}{c_p(T_w-T_\infty)}$ is the Eckert number, $S_r=\frac{D_m k_T(T_w-T_\infty)}{T_m\upsilon_f(C_w-C_\infty)}$ is the Soret number, $Lb=\frac{\upsilon_f}{D_m}$ is the bioconvection Schimdt number , $L_e=\frac{\upsilon_f}{D_B}$ is the Lewis number , $\gamma=\frac{k_0}{c}$ is chemical reaction parameter, $P_e=\frac{bW_c}{D_m}$ is the bioconvection Péclet number and $\Omega=\frac{N_\infty}{(N_w-N_\infty)}$ is the Microorganism concentration difference parameter. We also have $D_m, D_B, D_T, \tau=\frac{(\rho c)_p}{(\rho c)_f}$, which represents variable diffusivity of microorganisms, the Brownian diffusion coefficient, the thermophoresis diffusion coefficient, the ratio between the effective heat transfer capacity of the ultrafine nanoparticle material and the heat capacity of the fluid.

Here $s=\frac{v_w}{\sqrt{cv}}$ is the suction/injection parameter, $s\succ 0$ for suction and $s\prec 0$ for injection.
The nanoparticle volume fractions ϕ_1 and ϕ_2 are defined as:

$$\phi_1=(1-\phi)^{2.5}\left((1-\phi)+\phi\frac{(\rho)_s}{(\rho)_f}\right) \quad (25)$$

$$\phi_2=\frac{(\rho c_p)_{nf}}{(\rho c_p)_f}=(1-\phi)+\phi\frac{(\rho c_p)_s}{(\rho c_p)_f} \quad (26)$$

4. SOLUTION METHODOLOGY

In this section, the finite difference method is presented to solve the proposed model.

4.1. Computational Finite Difference Solutions

Now, we assume that $f_i, \theta_i, g_i, \varepsilon_i$ and Φ_i are the numerical solutions for the exact solutions $f, \theta, g, \varepsilon$ and Φ at the points $(\eta_i), i=0,\ldots,N$. The approximation formulations for f, θ, ϵ, g and Φ derivatives with respect to η are given as:

$$\left.\begin{aligned} g' &\simeq \frac{g_{i+1}-g_{i-1}}{2h}, \\ g'' &\simeq \frac{g_{i+1}-2g_i+g_{i-1}}{h^2}, \\ f' &\simeq \frac{f_{i+1}-f_{i-1}}{2h}, \\ f'' &\simeq \frac{f_{i-1}+f_{i+1}-2f_i}{h^2}, \\ f''' &\simeq \frac{-f_{i-2}+3f_{i-1}+f_{i+1}-3f_i}{h^3}, \\ \theta' &\simeq \frac{\theta_{i+1}-\theta_{i-1}}{2h}, \\ \theta'' &\simeq \frac{\theta_{i-1}+\theta_{i+1}-2\theta_i}{h^2}, \\ \varepsilon' &\simeq \frac{\varepsilon_{i+1}-\varepsilon_{i-1}}{2h}, \\ \varepsilon'' &\simeq \frac{\varepsilon_{i+1}-2\varepsilon_i+\varepsilon_{i-1}}{h^2}, \\ \Phi' &\simeq \frac{\Phi_{i+1}-\Phi_{i-1}}{2h}, \\ \Phi'' &\simeq \frac{\Phi_{i-1}+\Phi_{i+1}-2\Phi_i}{h^2}. \end{aligned}\right\} \quad (27)$$

Substituting (27) into (19-23) we get:

Momentum equation

$$\left((1+\frac{1}{\beta})+(1-\phi)^{2.5}K\right)\left(\frac{f_{i+1}+3f_{i-1}+f_{i-2}-3f_i}{h^3}\right) + \phi_1\begin{pmatrix} f_i\left(\frac{f_{i+1}-2f_i+f_{i-1}}{h^2}\right) \\ -\left(1+\frac{F_s}{D_a}\right)\left(\frac{f_{i+1}-f_{i-1}}{2h}\right)^2 \end{pmatrix} + K(1-\phi)^{2.5} \left(\frac{g_{i+1}-g_{i-1}}{2h}\right) + M(1-\phi)^{2.5}\left(E_1-\left(\frac{f_{i+1}-f_{i-1}}{2h}\right)\right) - \frac{1}{R_{ex}}\frac{1}{D_a}\left(\frac{f_{i+1}-f_{i-1}}{2h}\right)=0, \quad (28)$$

Angular momentum equation

$$\left(1+(1-\phi)^{2.5}\frac{K}{2}\right)\left(\frac{g_{i+1}-2g_i+g_{i-1}}{h^2}\right) + \phi_1\left(f_i\left(\frac{g_{i+1}-g_{i-1}}{2h}\right)-\left(\frac{f_{i+1}-f_{i-1}}{2h}\right)g_i\right) - (1-\phi)^{2.5}\phi_1 K\left(2g_i+\left(\frac{f_{i+1}-2f_i+f_{i-1}}{h^2}\right)\right) = 0. \quad (29)$$

Energy equation

$$(1-\phi)^{2.5}\left(\frac{\theta_{i+1}-2\theta_i+\theta_{i-1}}{h^2}\right)+ p_r\frac{k_f}{k_{nf}}\begin{pmatrix} \phi_2(1-\phi)^{2.5}f_i\left(\frac{\theta_{i+1}-\theta_{i-1}}{2h}\right)+ \\ (1-\phi)^{2.5}\begin{pmatrix} N_b\left(\frac{\theta_{i+1}-\theta_{i-1}}{2h}\right)\left(\frac{\Phi_{i+1}-\Phi_{i-1}}{2h}\right)+N_t\left(\frac{\theta_{i+1}-\theta_{i-1}}{2h}\right)^2+ \\ D_u\left(\frac{\Phi_{i+1}-2\Phi_i+\Phi_{i-1}}{h^2}\right) \end{pmatrix} \\ +E_c\left((1+\frac{1}{\beta})+(1-\phi)^{2.5}K\right)\left(\frac{f_{i+1}-2f_i+f_{i-1}}{h^2}\right)^2 \\ +(1-\phi)^{2.5}ME_c\left(\left(\frac{f_{i+1}-f_{i-1}}{2h}\right)-E_1\right)^2 \end{pmatrix}=0. \quad (30)$$

Gyrotactic microorganism equation

$$\left(\frac{\varepsilon_{i+1}-2\varepsilon_i+\varepsilon_{i-1}}{h^2}\right)+Lb\left(\frac{\varepsilon_{i+1}-\varepsilon_{i-1}}{2h}\right)f_i - P_e\begin{pmatrix}\left(\frac{\varepsilon_{i+1}-\varepsilon_{i-1}}{2h}\right)\left(\frac{\Phi_{i+1}-\Phi_{i-1}}{2h}\right) \\ +(\Omega+\varepsilon_i)\left(\frac{\Phi_{i+1}-2\Phi_i+\Phi_{i-1}}{h^2}\right)\end{pmatrix}=0, \quad (31)$$

Concentration equation

$$\left(\frac{\Phi_{i+1}-2\Phi_i+\Phi_{i-1}}{h^2}\right)+\frac{N_t}{N_b}\left(\frac{\theta_{i+1}-2\theta_i+\theta_{i-1}}{h^2}\right) + L_e\begin{pmatrix} f_i\left(\frac{\Phi_{i+1}-\Phi_{i-1}}{2h}\right)+\gamma\Phi_i \\ +S_r\left(\frac{\theta_{i+1}-2\theta_i+\theta_{i-1}}{h^2}\right)\end{pmatrix}=0. \quad (32)$$

Under conditions,

$$f_0=0, \frac{f_1-f_{-1}}{2h}=1, \theta_0=1, \Phi_0=1, \epsilon_0=1,$$
$$g_0=-n\,\frac{f_1-2f_0+f_1}{h^2}$$
$$\frac{f_{N+1}-f_{N-1}}{2h}=0, \frac{\theta_{N+1}-\theta_{N-1}}{2h}=0, \frac{\Phi_{N+1}-\Phi_{N-1}}{2h}=0,$$
$$\frac{\varepsilon_{N+1}-\varepsilon_{N-1}}{2h}=0, \frac{g_{N+1}-g_{N-1}}{2h}=0. \quad (33)$$

The system of equations (28)-(32) are solved numerically by using Mathematica package.

5. PHYSICALLY QUANTITIES

The skin friction coefficient is defined in terms of shear stress and density as:

$$, \qquad c_f=\frac{\tau_w}{\rho_{nf}u_w^2(x)} \quad (34)$$

Where is the surface shear stress defined as:

$$\tau_w = \left((\mu_B)_{nf}(1+\frac{1}{\beta}) + k^*\right)\left(\frac{\partial u}{\partial y}\right)_{y=0} + k^* N(y)_{y=0}. \quad (35)$$

The non-dimensional form of the local skin-friction coefficient is:

$$\phi_1 c_f = \sqrt{\frac{1}{R_{ex}}}\left[(1+\frac{1}{\beta}) + (1-n)(1-\phi)^{2.5}K\right] f''(0). \quad (36)$$

Where, $R_{ex} = \frac{ux}{\upsilon}$ is the local Reynolds number.

The couple stress at the surface is defined by

$$M_w = \left(\gamma^*_{nf}\frac{\partial N^*}{\partial y}\right)_{y=0} = \frac{(\mu_B)_f u_w}{\phi_1(1-\phi)^{2.5}}\left(1+(1-\phi)^{2.5}\frac{K}{2}\right) g'(0) \quad (37)$$

The Nusselt number is defined as:

$$Nu = \frac{xq_w}{k_f(T_w - T_\infty)}, \quad (38)$$

Where the wall heat flux is given as

$$q_w = -k_{nf}\left(\frac{\partial T}{\partial y}\right)_{y=0} \quad (39)$$

By using the above equations we can write the following dimensionless parameters:

$$-\theta'(0) = \frac{k_f}{k_{nf}}\sqrt{\frac{1}{R_{ex}}}Nu_x \quad (40)$$

The Sherwood number is defined as:

$$sh = \frac{xq_m}{D_B(C_w - C_\infty)} \quad (41)$$

where the wall mass flux, is presented as:

$$q_m = -D_B\left(\frac{\partial C}{\partial y}\right)_{y=0} \quad (42)$$

Applying the above equations, we can write:

$$-\Phi'(0) = \sqrt{\frac{1}{R_{ex}}}Sh_x. \quad (43)$$

The Density number of the motile micro-organism is defined as:

$$N_n = \frac{xq_n}{D_m(N_w - N_\infty)} \quad (44)$$

Where the flux and surface motile micro-organism has the form:

$$q_n = -D_m\left(\frac{\partial N}{\partial y}\right)_{y=0} \quad (45)$$

Using the above equation, we can write the local density number of motile micro-organism as:

$$-\varepsilon'(0) = \sqrt{\frac{1}{R_{ex}}}Nn_x. \quad (46)$$

6. RESULTS AND DISCUSSION

The objective of the present analysis is to study the non-Darcy electrically conducting of micropolar bi viscosity nanofluid behavior over a stretching sheet in the presence of viscous dissipation, Joule heating, and chemical reaction. The micropolar fluid contains four different types of nano-particles namely Copper (Cu), Silver (Ag), aluminum oxide (Al_2O_3) and Titanium dioxide (TiO_2) which are suspended in a blood-based fluid.The temperature and concentration fields are analyzed by utilizing the boundary layer concept. The set of coupled momentum, energy, and concentration equations is formulated mathematically by a system of non-linear partial differential equations (PDEs). A similarity transformation method is used to convert the nonlinear, coupled partial differential equations to a set of nonlinear coupled ordinary differential equations. These equations are solved numerically using the finite difference method technique. The effects of some important parameters of the present problem are examined. Also, the behavior of the nanoparticles Cu-nanoparticles, Ag-nanoparticles, Al_2O_3-nanoparticles and TiO_2-

nanoparticles are studied considering the given values $\phi = 0.05, 0.10, 0.15$ and 0.2 respectively.

Figure 1. Shows the velocity with respect to $\phi = 0.15, 0.2$ (Al_2O_3-nanoparticles, TiO_2d-nanoparticles) has elevated velocity values compared $\phi = 0.05, 0.10$ to Cu- nanoparticles and Ag- nanoparticles. This indicates that momentum for Al_2O_3-nanoparticles and TiO_2-nanoparticles is spreading faster inside the blood than propagating momentum for Cu-nanoparticles, Ag- nanoparticles. The anomalous of different nanoparticles through microorganism profiles studies in **Figure 2.** It is shown that the microorganisms profile decreases steeply for Al_2O_3-nanoparticles and TiO_2- nanoparticles when it is compared to Cu- nanoparticles, Ag- nanoparticles. The influence of different nanoparticles on the temperature profile is shown by **Figure 3:** It shows that from **Figure 3:** that the nanoparticles of TiO_2- nanoparticles are a good coolant in comparison to Ag-, Al_2O_3- nanoparticles, and Ag-nanoparticles. It shows that from **Figure 4:** that the concentration is highest in the case of Ag-nanoparticles as comparing with Al_2O_3-, and TiO_2-nanoparticles. It is depicted from **Figure 5:** that microrotation velocity diffuses faster in the case of Ag- nanoparticles and decreases in the case of TiO_2- nanoparticles.

Table 2: Shows the comportment of skin friction coefficient $(R_{ex})^{\frac{1}{2}}\phi_1 c_f$ for numerous values of E_1, F_S and K. It is perceived that the skin friction coefficient of all nanoparticles Cu, Ag, Al_2O_3 and TiO_2 is a decreasing function of E_1 and K. The applied electric field introduces accelerating body force which acts to the direction of the applied electric field. This body force, known as the Lorentz force, accelerates the boundary layer flow and thickens the momentum boundary layer. Hence it resulted in a reduction in the skin friction at the stretching surface. Moreover, the fact behind the decreasing of the skin friction coefficient with material parameter is that the micropolar fluids offer a greater resistance (resulting from dynamic viscosity and vortex viscosity) to the fluid motion. On the other hand the skin friction coefficient is an increasing function of F_S the reason behind this fact is that porous medium gives rise to skin friction coefficient. From this

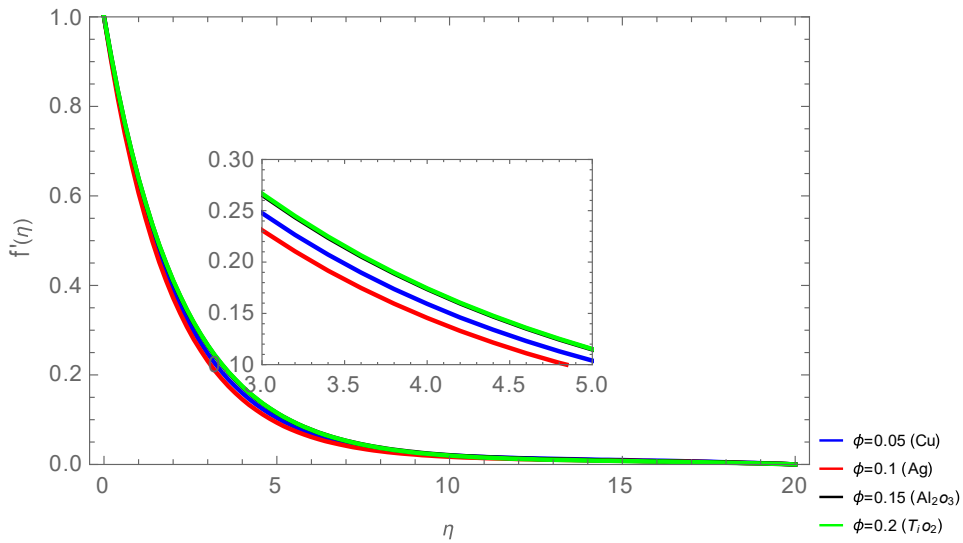

Figure 1. Behavior of $f'(\eta)$ for various values of ϕ when $D_u = 0.4, n = 0.001, \Omega = \gamma = M = 0.01 F_s = L_e = P_e = R_{ex} = D_a = Nb = Nt = E_c = \beta = E_1 = s = P_r = S_r = L_b = 0.2$ and $K = 1$

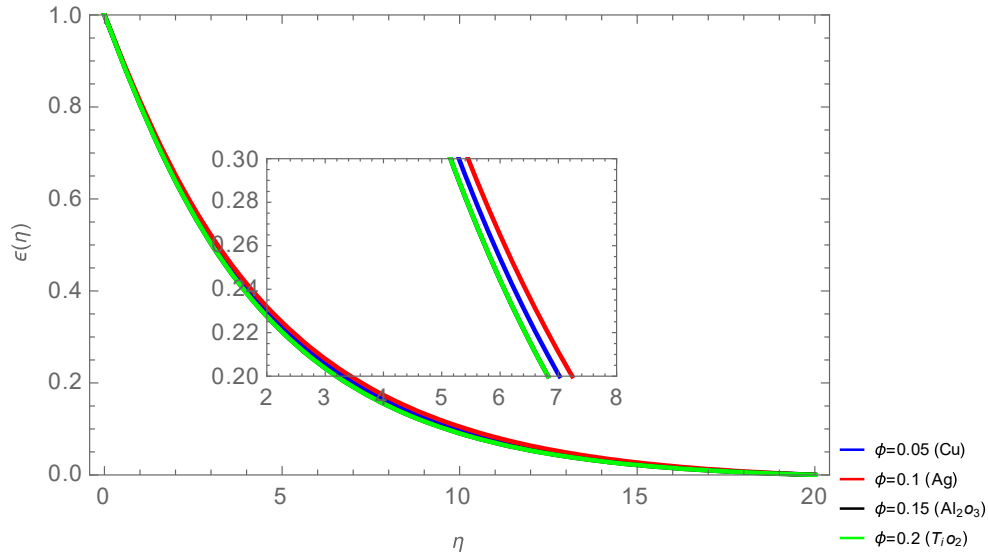

Figure 2. Behavior of $\varepsilon(\eta)$ for various values of ϕ when $D_u = 0.4, n = 0.001, \Omega = \gamma = M = 0.01 F_s = L_e = P_e = R_{ex} = D_a = Nb = Nt = E_c = \beta = E_1 = s = P_r = S_r = L_b = 0.2$ and $K = 1.5$.

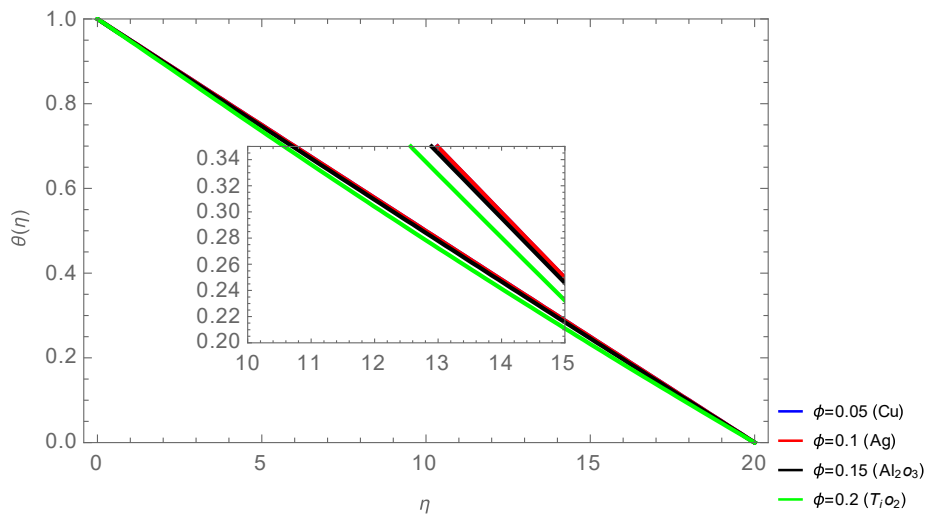

Figure 3. Behavior of $\theta(\eta)$ for various values of ϕ when $D_u = 0.4, n = 0.001, \Omega = \gamma = M = 0.01 F_s = L_e = P_e = R_{ex} = D_a = Nb = Nt = E_c = \beta = E_1 = s = P_r = S_r = L_b = 0.2$ and $K = 1.5$.

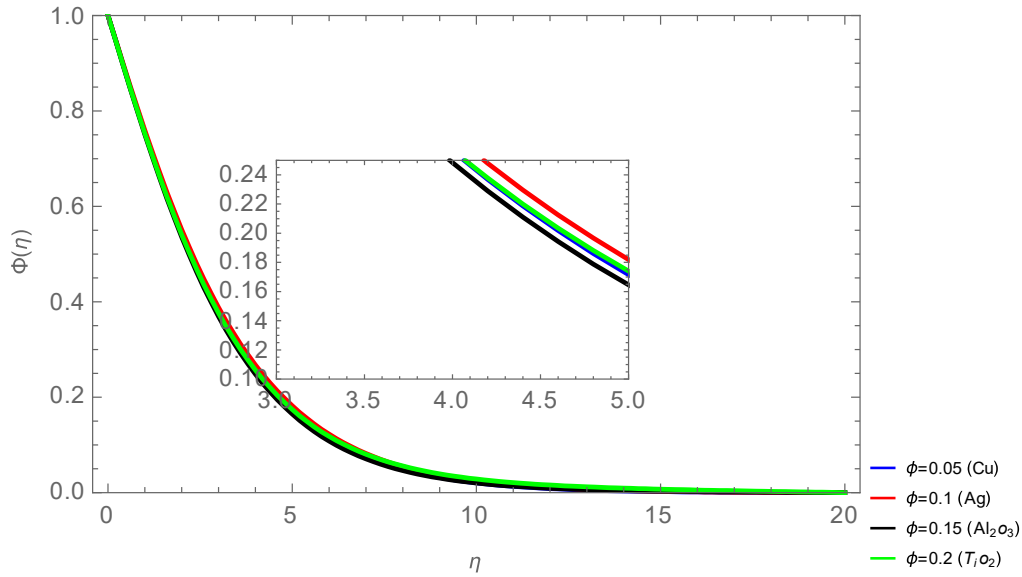

Figure 4. Behavior of $\Phi(\eta)$ for various values of ϕ when $D_u = 0.4, n = 0.001, \Omega = \gamma = M = 0.01 F_s = L_e = P_e = R_{ex} = D_a = Nb = Nt = E_c = \beta = E_1 = s = P_r = S_r = L_b = 0.2$ and $K = 1.5$.

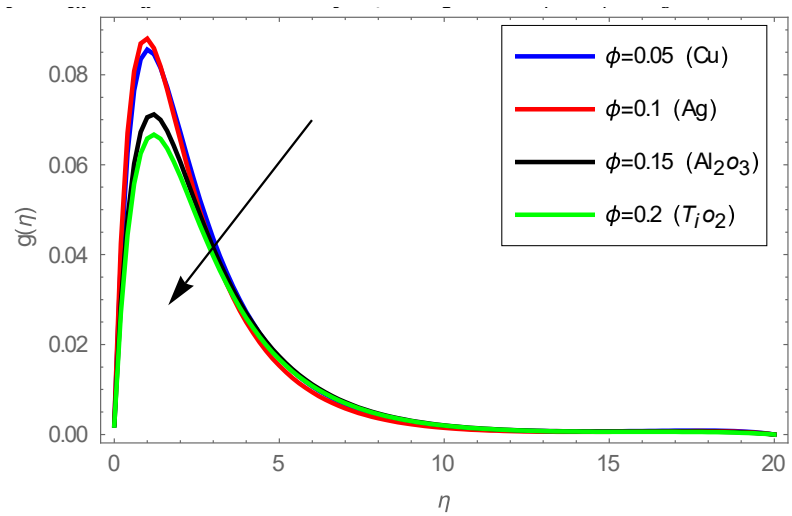

Figure 5. Behavior of $g(\eta)$ for various values of ϕ when $D_u = 0.4, n = 0.001, \Omega = \gamma = M = 0.01 F_s = L_e = P_e = R_{ex} = D_a = Nb = Nt = E_c = \beta = E_1 = s = P_r = S_r = L_b = 0.2$ and $K = 1.5$.

Table 2. Behavior of skin friction coefficient $(R_{ex})^{\frac{1}{2}}\phi_1 c_f$ for four types of nanofluids when $M = F_s = L_e = P_e = 0.2, n = \gamma = \Omega = 0.01, Nb = Nt = E_c = \beta = E_1 = s = P_r = S_r = L_b = 0.1,$ $R_{ex} = 2, D_u = 0.4$ and $K = 1.5$.

$$(R_{ex})^{\frac{1}{2}}\phi_1 c_f = -\left((1+\frac{1}{\beta})f''(0) + (1-n)(1-\phi)^{2.5}Kf''(0)\right)$$

		Cu	*Ag*	Al_2O_3	TiO_2
E_1	0.5	0.462532	0.491366	0.440949	0.438778
	1.0	0.446912	0.478969	0.429061	0.430286
	1.5	0.431644	0.465264	0.416036	0.420451
F_s	0.5	0.506383	0.535832	0.487047	0.474076
	1.0	0.566573	0.613973	0.539300	0.534252
	1.5	0.628842	0.673677	0.591048	0.583160
K	0.5	0.482238	0.509613	0.466050	0.461816
	1.0	0.472176	0.500333	0.458587	0.447550
	1.5	0.462532	0.491929	0.451706	0.441746

table we also notice that, the nano-particles of Ag has the higher skin friction coefficient rather than Cu, TiO_2 and Al_2O_3 nanoparticles.

Table 3: display the comportment of the local density number of motile micro-organisms $(R_{ex})^{\frac{1}{2}}\varepsilon'(0)$. It shows that the local density number of motile micro-organisms $(R_{ex})^{\frac{1}{2}}\varepsilon'(0)$ is increasing function of P_e, Lb and Ω for Cu, Ag, Al_2O_3 and TiO_2 nano-particles. As expected an increase in the motile micro-organisms flux is noted with bioconvection Péclet number P_e and the micro-organisms concentration difference parameter Ω. This would be attributed to the fact that the concentration of motile micro-organisms within the boundary layer for motile micro-organisms decreases as these parameters increase. Additionally when bioconvection Schimdt number Lb increase means that thermal diffusivity prevails against mass diffusivity, these two facts prove the physical reason behind the increasing density number of motile micro-organisms with bioconvection Schimdt number , bioconvection Péclet number P_e and the micro-organisms concentration difference parameter Ω for all nano-particles. Also, it is perceived that from this table the magnitude of motile micro-organisms in the case of TiO_2 nano-particles achieves higher value than other nano-particles (Ag, Al_2O_3 and Cu).

Figure 6 depicts the effect of the microorganism's concentration difference parameteron the density of motile microorganisms' profile. It observed that an increase in microorganism's concentration difference parameter Ω tends to decrease the density of motile microorganisms. **Figure 7** displays the behavior of the bioconvection Lewis number Lb against the density of motile microorganisms' profile. An increase in the value of Lb contribute to a decrease in the diffusion of microorganisms. Ultimately, the thickness of the boundary layer decreases along with the density of the motile microorganisms. The profile of angular velocity is $g(\eta)$ shown in **Figure 8** for various values of material parameter K. It is shown that, as expected increase with increasing material parameter K. Of course, when the viscosity of the fluid decreases the angular velocity of additive increases.

Table 3. Behavior of local density number of motile micro-organism $(R_{ex})^{\frac{1}{2}}\varepsilon'(0)$ for four types of nano fluids when $M = F_s = L_e = P_e = 0.2, n = \gamma = \Omega = 0.01, Nb = Nt = E_c = \beta = E_1 = s = P_r = S_r = L_b = 0.1, R_{ex} = 2, D_u = 0.4$ and $K = 1.5$.

$-\varepsilon'(0) = \sqrt{\frac{1}{R_{ex}}} Nn_x$					
		Cu	*Ag*	Al_2O_3	TiO_2
P_e	0.2	0.205630	0.200703	0.202734	0.207385
	0.8	0.331247	0.324375	0.328520	0.333259
	1.5	0.479857	0.470520	0.476412	0.481709
L_p	0.1	0.205630	0.200703	0.202734	0.207358
	0.8	0.646163	0.639602	0.647347	0.650645
	1.5	0.904750	0.898097	0.906092	0.909148
Ω	0.01	0.205630	0.200703	0.202734	0.207385
	0.5	0.224556	0.219401	0.221963	0.226393
	1.0	0.243868	0.238481	0.241491	0.245715

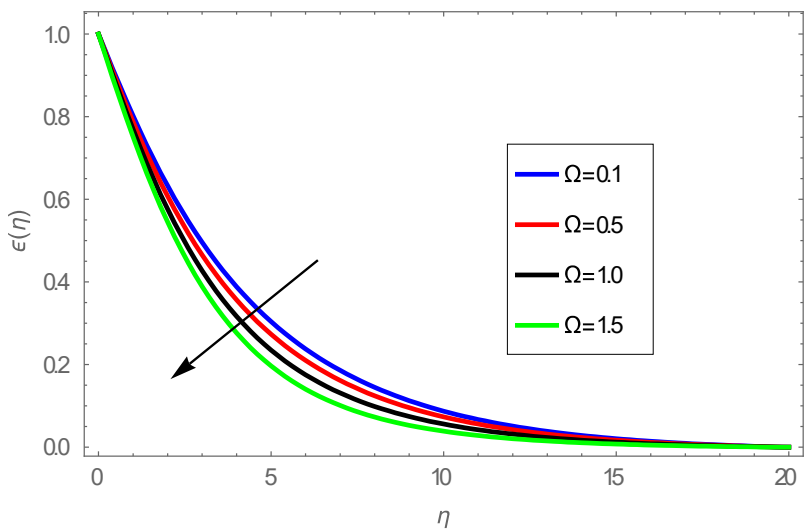

Figure 6. Behavior of $\varepsilon(\eta)$ for various values of Ω when $D_u = 0.4, n = 0.001, \phi = 0.05, \gamma = M = 0.01, F_s = L_e = P_e = R_{ex} = D_a = Nb = Nt = E_c = \beta = E_1 = s = P_r = S_r = L_b = 0.2$ and $K = 1.5$.

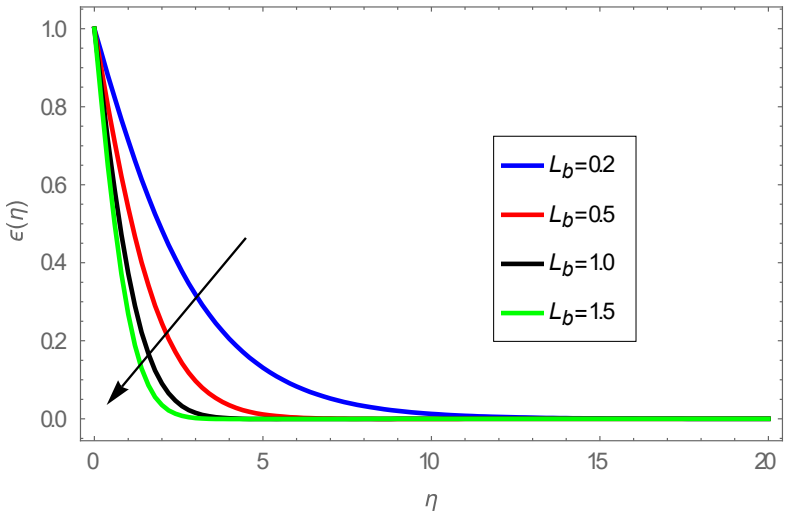

Figure 7. Behavior of $\varepsilon(\eta)$ for various values of L_b when $D_u = 0.4, n = 100, \gamma = M = 0.01, F_s = L_e = P_e = R_{ex} = D_a = Nb = Nt = E_c = \beta = E_1 = s = P_r = S_r = 0.2, \Omega = 0.1$ and $K = 1.5$.

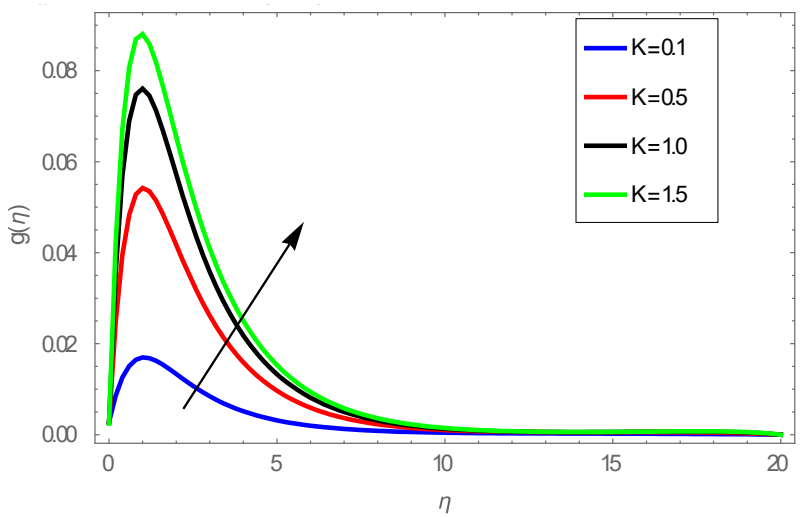

Figure 8. Behavior of $g(\eta)$ for various values of K when $D_u = 0.4, n = 100, \gamma = M = 0.01, F_s = L_e = P_e = R_{ex} = D_a = Nb = Nt = E_c = \beta = E_1 = s = P_r = S_r = L_b = 0.2$ and $\Omega = 0.01$.

Figure 9 demonstrates typical profiles for the dimensionless velocity $f'(\eta)$, the angular velocity $g(\eta)$, the density of motile microorganisms $\varepsilon(\eta)$ and the concentration $\Phi(\eta)$ for various values of the bi-viscosity parameter β, respectively. As expected, $f'(\eta)$ decrease while $g(\eta)$, $\varepsilon(\eta)$ and $\Phi(\eta)$ increase with increasing bi-viscosity parameter β. The behavior of Forchheimer number F_S on the dimensionless velocity $f'(\eta)$, the angular velocity $g(\eta)$, the density of motile microorganisms $\varepsilon(\eta)$ and the concentration $\Phi(\eta)$ are illustrated in **Figure 10**. It is noticed that the velocity decrease whilst the angular velocity, the density of motile microorganisms and the concentration increase with increasing Forchheimer number F_S. **Figure 11** demonstrates typical profiles for the dimensionless velocity $f'(\eta)$, the angular velocity $g(\eta)$, the density of motile microorganisms $\varepsilon(\eta)$ and the concentration $\Phi(\eta)$ for various values of Dufour number D_U. It is observed that the velocity increase whilst the angular velocity, the density of motile microorganisms and the concentration decrease with increasing Duffor number D_U.

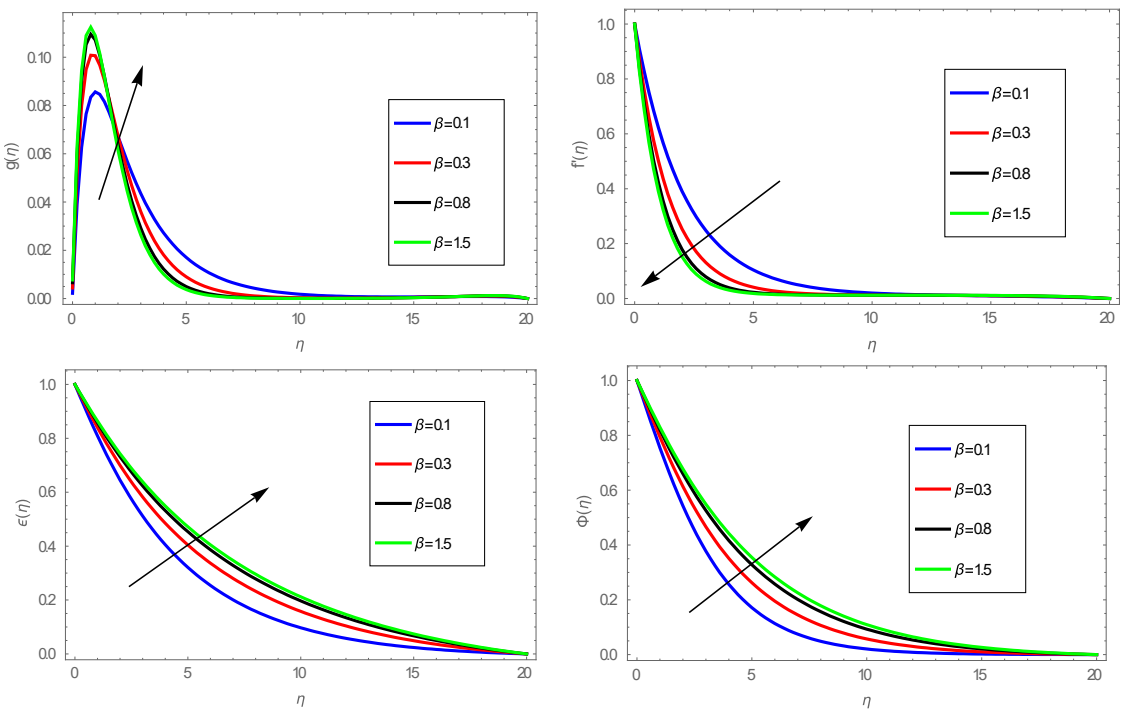

Figure 9. Behavior of $f'(\eta)$,$g(\eta)$, $\varepsilon(\eta)$ and $\Phi(\eta)$ for various values of β when $D_u = 0.4, n = 100, \gamma = M = 0.01, K = 1.5, L_e = P_e = F_s = D_a = Nb = Nt = E_c = R_{ex} = E_1 = s = P_r = S_r = L_b = 0.2$ and $\Omega = 0.01$.

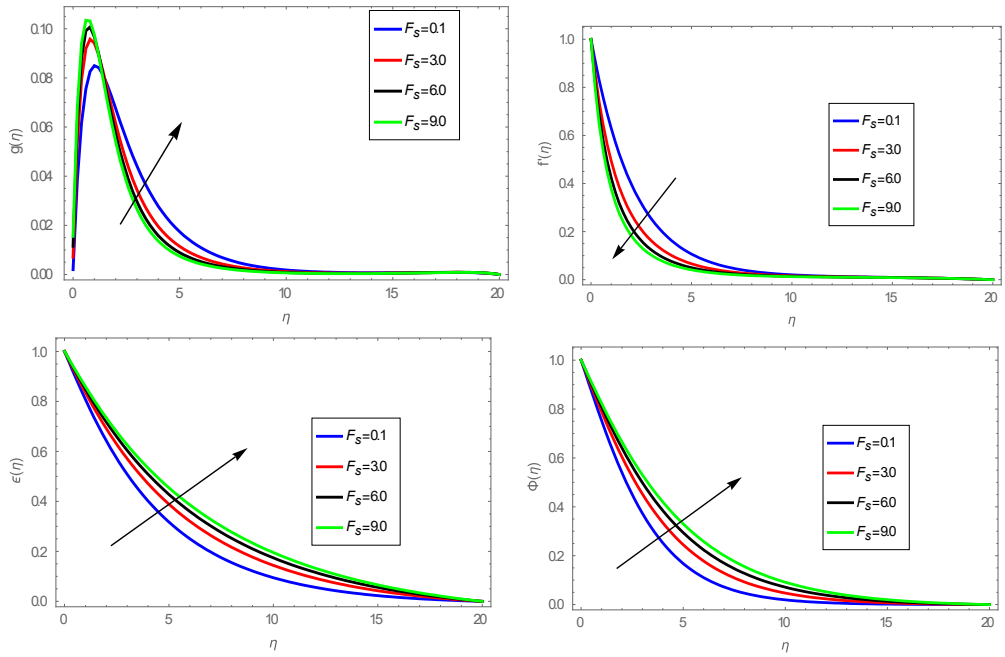

Figure 10. Behavior of $f'(\eta)$,$g(\eta)$, $\varepsilon(\eta)$ and $\Phi(\eta)$ for various values of F_s when $D_u = 0.4, n = 100$, $\gamma = M = 0.01, K = 1.5, L_e = P_e = R_{ex} = D_a = Nb = Nt = E_c = \beta = E_1 = s = P_r = S_r = L_b = 0.2$ and $\Omega = 0.01$.

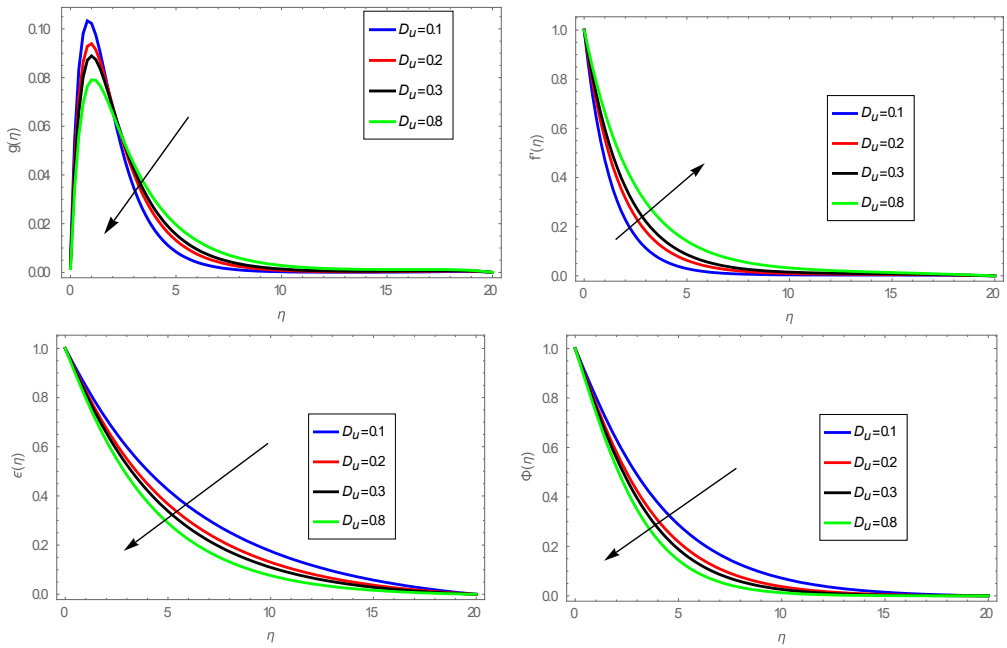

Figure 11. Behavior of $f'(\eta)$,$g(\eta)$, $\varepsilon(\eta)$ and $\Phi(\eta)$ for various values of D_u when $\beta = 0.1, n = 1 = M = 0.01, K = \gamma = L_b = 0.2 and \Omega = 0.011.5, L_e = P_e = F_s = D_a = Nb = Nt = E_c = R_{ex} = E_1 = s = P_r = S_r 00, \phi = 0.05$,

7. Conclusions

This paper has presented a study of the more complicated problem which involves both the heat and mass transfer of the non-Darcian boundary layer flow of electrical magnetohydrodynamic micropolar bioviscosity nanofluid containing Gyrotactic Microorganisms over a stretching surface. Four different types of nano-particles namely Copper (Cu), Silver (Ag), aluminum oxide (Al_2O_3) and Titanium dioxide (TiO_2) are suspended in a blood-based nanofluid by taking into account the Soret and Dufour effects. A similarity transformation was employed to change the governing partial differential equations into ordinary ones. These equations were solved numerically by using finite difference method. The numerical results indicate that:

• The nano-particles of Ag has the higher skin friction coefficient $(R_{ex})^{\frac{1}{2}}\phi_1 c_f$ rather than Cu, TiO_2 and Al_2O_3 nano-particles.

• The magnitude of density motile microorganisms $(R_{ex})^{\frac{1}{2}}\varepsilon'(0)$ in the case of Cu nano-particles achives higher value than other nano-particles (Ag, Al_2O_3 and TiO_2).

• The momentum for (Al_2O_3-nanoparticles, TiO_2-nanoparticles) is spreading faster inside the blood than propagating momentum for (Cu-nanoparticles, Ag-nanoparticles).

• The nanoparticles of TiO_2- nanoparticles are a good coolant in comparison to Ag-, Al_2O_3-, and Ag-nanoparticles.

• The microrotation velocity diffuses faster in the case of Ag-nanoparticles and decreases in the case of TiO_2-nanoparticles.

• The velocity decrease whilst the angular velocity, the density of motile microorganisms and the concentration increases with increasing Forchheimer number F_S.

Acknowledgements

Authors are grateful to the respected referees for their valuable remarks and constructive suggestions which significantly contributed the quality of the paper.

Conflict of interest statement

The author declare that there is no conflict of interest.

References

[1] Abdelsalam S.I., Mekheimer Kh.S., and Zaher A.Z., *Chinese J. Phys.*, 2020; **67:** 314-329. DOI 10.1016/j.cjph.2020.07.011

[2] Das S.K., Choi S.U.S., Wenhua Yu. and Pradeep T., *Nanofluids: Science and Technology*, 1st Edn., John Wiley and Sons, USA, 2007.

[3] Sheikholeslami M., Hayat T. and Alsaedi A., *Int. J. Heat Mass Tran.,* 2016; **96:** 513-524. DOI 10.1016/j.ijheatmasstransfer.2016.01.059.

[4] Azizah M., Syakila A. and Pop, I., *Int. J. Heat Mass Tran.,* 2011; **55:** 1888-1897. DOI 10.1016/j.ijheatmasstransfer.2011.11.042.

[5] Hamad M.A.A., *Int. Commun. Heat Mass,* 2011; **38:** 487-492. DOI 10.1016/j.icheatmasstransfer.2010.12.042.

[6] Nazar R., Tham L., Pop I. and Ingham D.B., *Transport Porous Med.,*2011; **86:** 517-536. DOI 10.1007/s11242-010-9637-1.

[7] Yacob N.A., Ishak A., Nazar R. and Pop I., *Nanoscale Res. Lett.,* 2011; **6:** 1-7. DOI 10.1186/1556-276X-6-314.

[8] Kuznetsov A.V. and Avramenko A.A., *Int. Commun. Heat Mass,* 2004; **31:** 1-10. DOI 10.1016/S0735-1933 (03)00196-9.

[9] Kuznetsov A.V., *Nanoscale Res. Lett.*, 2011; **6:** 100. DOI 10.1186/1556-276X-6-100.

[10] Alsaedi A., Khan M.I., Farooq M., Gull N. and Hayat T., *Adv. Powder Technol.*; 2017, **28**: 288-298. DOI 10.1016/j.apt.2016.10.002.

[11] Zohra F., Uddin M., Ismail A., Bég O.A. and Kadir A., *Chinese J. Phys.,* 2018, **56**: 432-448. DOI 10.1016/j.cjph.2017.08.031.

[12] Vadasz P., *Emerging Topics in Heat and Mass Transfer in Porous Media: From Bioeengineering*

and Microelectronics to Nanotehnology, 1st Edn., Springer, Netherland, 2008.

[13] Eringen A.C., *Micro continuum Field Theories: II. Fluent Media,* 1st Edn., Springer-Verlag, New York, 2001.

[14] Lok Y.Y., Amin N. and Pop L., *Int. J. Therm. Sci.,* 2003; **42(11):** 995-1001. DOI 10.1016/S1290-0729(03)00079-6.

[15] Sandeep N. and Sulochana C., *Eng. Sci. Technol.,* 2015; **18(4)**: 738-745. DOI 10.1016/j.jestch.2015.05.006 .

[16] Rahman M. and Sultana T., *Nonlinear Anal.-Model.,* 2008; **13(1):** 71-78. DOI 10.15388/NA.2008.13.1.14590.

[17] Postelnicu A., *Int. J. Heat Mass Tran.,* 2004; **47:** 1467-1472. DOI 10.1016/j.ijheatmasstransfer.2003.09.017.

[18] Partha M.K., Murthy P.V.S.N. and Raja Sekhar G.P., *J. Heat Trans-T. ASME,* 2006; **128(6):** 605-610. DOI 10.1115/1.2188512.

[19] Mansour A., Amahmid A., Hasnaoui M. and Bourich M., *Numer. Heat Tr. A-Appl.,* 2006; **49(1):** 69-94. DOI 10.1080/10407780500302166.

[20] Lakshmi Narayana P.A. and Murthy P.V.S.N., *J. Porous Media,* 2007; **10(6):** 613-623. DOI 10.1615/JPorMedia.v10.i6.70.

[21] Lakshmi Narayana P.A., Murthy P.V.S.N., *J. Heat Trans-T. ASME,* 2008; **130(10):** 104504-1–104504-5. DOI 10.1115/1.2789716.

[22] Brinkman H.C., *J. Chem. Phys.,* 1952; **20(4):** 571-581. DOI: 10.1063/1.1700493.

[23] Nakamura M. and Sawada T., *J. Biomech. Eng.,* 1988; **110(2):** 137-143. DOI 10.1115/1.3108418.

[24] Mekheimer K.h.S., Zaher A.Z. and Hasona W.M., *Chinese J. Phys.,* 2020; **65:** 123-138. DOI 10.1016/j.cjph.2020.02.020.